Title: Histological structure of baleen plates and its relevance to sampling for stable isotope studies

Authors: Diego Rita[1*], Asunción Borrell[1], Gísli Víkingsson[2], Alex Aguilar[1]

Affiliations:

[1] Institute of Biodiversity Research (IRBio) and Department of Evolutionary Biology, Ecology and Environmental Sciences, University of Barcelona, Barcelona. P.C. 08028. Spain.

DR: diegorita@ub.edu

AB: xonborrell@ub.edu

AA: aaguilar@ub.edu

[2] Marine and Freshwater Research Institute, Reykjavík. P. O. Box 1390

GV: gisli.vikingsson@hafogvatn.is

Corresponding author:

Diego Rita: Department of Evolutionary Biology, Ecology and Environmental Sciences. Faculty of Biology. University of Barcelona. P.C. 08026. Spain; Email address: diegorita@ub.edu

Abstract: Stable isotope analysis of baleen plates is a widespread technique for studying baleen whales. Typically, subsamples along the growth axis of the baleen plate are extracted and analysed to examine time-related variation in their stable isotope signals. However, baleen plate tissue is composed of two different tissues: a pair of cortex layers flanking an internal medulla. These two histological components exhibit differential development, and their consolidation as a tissue is therefore likely non-synchronic. This could influence stable isotope results because the stable isotope signal may differ in each subsample according to the proportion of the two histological components extracted from the tissue. In this study, stable isotope analysis was combined with optical microscopy examination of fin whale (*Balaenoptera physalus*) baleen plates to understand the ontogeny of the two histological components. In both of them, the $\delta^{15}N$ values followed a sinewave pattern along the growth axis of the baleen plate. However, the $\delta^{15}N$ values of the cortex appeared to be advanced compared to those of the medulla. Additionally, the amplitude of the $\delta^{15}N$ values in the oscillations was higher in the cortex than in the medulla. The histological examination revealed that these differences are caused by earlier and faster synthesis of the cortex layer compared to that of the medulla. Because the stable isotope ratios of the two layers differ, we propose that in this type of studies only the outer-most part (closest to

the surface) of the cortex should be subsampled and analysed. Additionally, to include the most recently formed tissue, this subsampling should start well below the zwischensubstanz, or baleen “gum”.

Keywords: Stable isotopes; *Balaenoptera physalus*, Baleen plate; Histology; Mysticete

Introduction

Stable isotope ratios are widely used chemical tracers in animal ecology studies (Hobson, 1999; Peterson and Fry, 1987). These ratios provide information on a number of biological traits, such as the foraging ecology (Clementz and Koch, 2001), migration patterns (Bowen et al., 2005) and/or behavioural specialization of individuals (Bond et al., 2016; Rita et al., 2017). Metabolically inert tissues, such as whiskers, nails and hairs, are of particular relevance for this type of study. These tissues are formed by high-turnover stem cells that rapidly acquire the stable isotope ratios of the body pool (Ayliffe et al., 2004; Fry and Arnold, 1982). Once formed, their composition is fixed, and they do not exchange materials with the rest of the body, thus preserving a permanent and invariable record of the signal (Rubenstein and Hobson, 2004). Furthermore, tissues of this type that grow continuously store a time-series record of the stable isotope ratios of the body pool at various stages of the life cycle (Rubenstein and Hobson, 2004). In mysticetes, one such tissue that has proven particularly useful and has been the subject of numerous studies is the baleen plate (Busquets-Vass et al., 2017; DeHart and Picco, 2015; García-Vernet et al., 2018; Ryan et al., 2013).

The baleen plate is a keratinous tissue that grows on the upper jaw of all mysticetes (Rice, 2002). Its growth is continuous throughout the lifespan, and the longest plates of some individuals preserve information that covers over a decade in the case of balaenids (Hobson and Schell, 1998) or a few years in the case of balaenopterids (Aguilar et al., 2014). Typically, the stable isotopes of the baleen plates present annual oscillation due to prey switching, a change in baseline stable isotopes or fasting along the annual migratory route. However, there is no standardized method for baleen plate subsampling, and different studies may use different techniques. In some cases, baleen plate subsampling is performed by scraping off a thin layer of the baleen plate surface; in others, a hole is drilled through the plate (Bentaleb et al., 2011; Busquets-Vass et al., 2017; Hunt et al., 2016; Mitani et al., 2006), and many studies do not specify the technique used (Eisenmann et al., 2016; Giménez et al., 2013; Hobson et al., 2004; Matthews and Ferguson, 2015). Different subsampling methods are likely to collect different components of the baleen plate since the baleen plate is not a homogenous tissue, potentially impacting the reliability and comparability of the results.

Baleen plates are composed of two histological components with a sandwich-type arrangement (Fig 1). The medulla (the interior layer) consists of horny tubules that run

parallel to the growing axis of the plate. The walls of these horny tubules are composed of concentric rings of flat and keratinized cells (Fig 1) and, in some cases, calcium (Pfeiffer, 1992). The interior of the tubules, on the other hand, is filled with connective tissue near the base of the plate, but it may be empty in a mature plate (Pfeiffer, 1992). The medulla is flanked by two sheets of cortex (Fig 1) composed of compact keratin filaments and flat cells (Fudge et al., 2009). During the early growth stages of the baleen plate, the medulla and the cortex sheets are separated by a third layer (Van Utrecht, 1966), which could play a role in the development of the other two layers. All histological components are synthesised inside the baleen "gum", or zwischensubstanz (Pinto and Shadwick, 2013; Van Utrecht, 1966; Young et al., 2015) (a white rubbery tissue that supports the base of the baleen plates). However, the exact depth at which the synthesis of each component occurs, where the tissue becomes completely keratinized, ("origin point" hereafter) is unknown. Previous histological studies have shown that the synthesis of the cortex occurs before that of the medulla (Van Utrecht, 1966), and this lack of synchronicity in tissue formation may cause a lag between the stable isotope ratios of the two components at any given tissue location.

The baleen plates used in this study belonged to two fin whales (*Balaenoptera physalus*) from the Icelandic population. This population feeds near Iceland during the boreal summer and migrates to lower latitudes of the North Atlantic during winter, a shift that is known to imprint an oscillatory pattern on the stable isotope ratios along the baleen plate growth axis (Aguilar et al., 2014; García-Vernet et al., 2018). The baleen plates of fin whales may include up to three of these oscillations since they grow at a rate of 18–23 cm (mean =20 cm)·year^{-1} and measure up to 60 cm in length (Aguilar et al., 2014). These oscillations can be used to cross-correlate the isotopic signals of the two baleen plate layers to detect any time lag between the two layers.

The aim of the present study was to examine the process of the synthesis of the baleen plate components and the consequences that this process may have on the subsampling of the tissue. This new information may help to improve the accuracy and replicability of studies on stable isotope ratios in baleen plates. To this end, we performed histological examinations and stable isotope analysis at subsampling points along the growth axis of the baleen plates.

Material and methods

Sample collection

The baleen plates analysed in this study were obtained from two fin whales that were captured during commercial whaling operations in Iceland in 2015: whale #81, a juvenile 16.5-metre male caught at 64º25´N-28º02'W; and whale #97, a 19.2-metre female pregnant with a 134-centimetre foetus, caught at 64º00´N-27º48'W. One baleen plate collected from the middle section of the right jaw was excised from each animal at the very proximal end, in contact with the jawbone, to ensure that the whole plate had been sampled. The plate of whale #97 measured 67 cm, and the plate of whale #81 measured 63 cm. The plates were kept frozen at -20º C until analysis.

Histological sections

From each baleen plate, we excised two stripes running parallel to the growing axis of the plate, one along and near the labial margin and the other along and near the lingual margin. The width of each stripe was 1 cm. Then, each of them was cut at distances of 1 cm, thus obtaining 1 cm x 1 cm square samples (Fig 2). After concluding the process of synthesis, the histological structure of the plate remains essentially unaltered with the passing of time. Therefore, we focused our study on the synthesis portion of the baleen plate, which is the one located mostly underneath the baleen "gum" (zwischensubstanz) and, consequently, the histological examination of this portion was made in greater detail. Thus, the sampling consisted of one sample every centimetre in the region of the baleen plate inside the "gum" and one every 10 cm in the rest of the baleen plate (Fig 2). Each sample, which had been kept frozen during the cutting process, was subsequently immersed for 24 h in 4% formaldehyde to preserve the histological structure; 4% formaldehyde and 30% sucrose to maintain the preservation process and initiate cryoprotection; 40 mM phosphate-buffered saline and 30% sucrose to extract the excess formaldehyde from the samples; and cryoprotectant solution (30% glycerol, 30% ethylene glycol in phosphate buffer 0.1 M) to further protect the histological samples from the cold temperatures of the cryostat. Then, the samples were frozen using dry ice, and histological sections were obtained using a cryostat. From each sample, several 20 µm-thick histological sections were cut perpendicular to the growing axis of the plate.

The sections from the samples of the labial strip of the plate from whale #81 were stained using haematoxylin-eosin. However, better results were obtained using

Mallory's trichrome technique; therefore, the remaining samples (i.e., the lingual strip of the plate from whale #81 and both strips of the plate from whale #97) were stained using that technique. These two staining techniques were chosen because they are standard methods that have consistently proven to be useful for observation of the baleen plate tissue (i.e. Van Utrecht, 1966).The first staining technique only discriminated the basic cell components from the acidic cell components, such as the nucleus from the cytoplasm, while the Mallory technique stained collagen, keratin and cytoplasm with different colours.

During the histological examination, we observed that the cortex and the horny tubules of the medulla were extremely thin at the base of the plate and became thicker at more distal positions until they reached their maximum thickness in the fully developed plate. Thus, we decided to use the width of the cortex and the width of the medullar tubules as proxies of cortex development and medulla development, respectively (Fig 1). Cortex width, tubule diameter and tubule lumen diameter were measured in each subsample using an ocular micrometre under the optic microscope. Tubule wall width was calculated as the difference between the tubule radius and the tubule lumen radius. Each measurement was repeated in different sections from each sample (a minimum of seven measurements were conducted for each sample, but 20 measurements were performed when possible). The results reported here are the mean of all the measurements of one subsample. For further details, including the standard deviations obtained along the measurements, see Supplementary Data SD1.

Stable isotope analysis

Nitrogen and carbon stable isotope ratios were analysed from the lingual and labial sides of the baleen plates. Before drilling the baleen plate subsamples, the "gum" was removed using a scalpel, and the plate surface was rinsed using chloroform/methanol (2:1) solution. This removed possible surface lipids that might impact the measured isotopic values. Subsamples were collected from the zone inside the "gum" at adjacent locations to those subjected to histological examination and from the zone outside the "gum" every 1 cm along the first 10 centimetres of the emerged plate (Fig 2). A Dremel 300 series drill was used to obtain powder from the cortex of the plate by carefully scratching its surface. For the medulla samples, the cortex was removed using the drill until the medulla tubules could be seen, and after rinsing with 96% ethanol, the medulla was scratched using the drill. To ensure that only medulla was sampled, the path

carved in the cortex was wide enough to guarantee that the drill tip would not touch the cortex walls of the path while sampling the medulla.

Approximately 0.3 mg of baleen keratin was weighed into tin cups (3.3 x 5 mm) and analysed along with calibration standards by elemental analysis isotope ratio mass spectrometry (EA-IRMS) using an elemental analyser (model FlashEA 1112, ThermoFisher Scientific) coupled with a Delta C isotope ratio mass spectrometer (ThermoFinnigan). All analyses were performed at the Scientific and Technological Centre (CCiT) of the University of Barcelona.

Nitrogen stable isotope abundances are expressed in delta (δ) notation, with relative variations of stable isotope ratios expressed in per mil (‰) deviations from predefined international standards (Bond and Hobson, 2012). The international standards used were atmospheric nitrogen (air) for $\delta^{15}N$ and Vienna Pee Dee Belemnite (VPDB) calcium carbonate for $\delta^{13}C$. However, the data were normalized using commercially available laboratory reference materials. Secondary isotopic reference materials of known ^{15}N:^{14}N ratios, as given by the International Atomic Energy Agency (IAEA, Vienna, Austria), were used for calibration at a precision of 0.05%. These materials included $(NH_4)_2SO_4$ (IAEA-N-1, $\delta^{15}N$ = +0.4 ‰ and IAEA-N-2, $\delta^{15}N$ = +20.3 ‰), L-glutamic acid (IAEA USGS-40, $\delta^{15}N$= -4.5 ‰) and KNO_3 (IAEA-N-3, $\delta^{15}N$= +4.7 ‰). For carbon, the secondary isotopic reference materials with known ^{13}C:^{12}C ratios included polyethylene (IAEA-CH-7, $\delta^{13}C$ = -32.1‰), L-glutamic acid (IAEA USGS-40, $\delta^{13}C$ = -26.4 ‰) and sucrose (IAEA-CH-6, $\delta^{13}C$ = -10.4 ‰). These isotopic reference materials were assessed once per 12 analysed samples to recalibrate the system and compensate for any measurement drift over time. The raw data were normalized by the multipoint normalization method based on linear regression (Skrzypek, 2013).

The results regarding carbon stable isotope values lacked the standard and well-defined oscillation pattern that is necessary to carry out cross-correlation analysis. For this reason, only the nitrogen stable isotope values were used for the statistical analysis. For further details on the stable isotope values of carbon and nitrogen, see Supplementary Data SD2.

Statistical analysis

All statistical analyses were carried out using the free software R (R Core Team, 2016). The lag between the stable isotope ratios of the baleen cortex and the baleen medulla was statistically calculated via cross-correlation. The peak-to-valley amplitude

(hereafter referred to as the amplitude) was calculated as the difference between the maximum and minimum $\delta^{15}N$ value of an oscillation.

The origin point of the cortex was estimated for each strip by fitting a linear regression between the cortex width values and the distance to the base of the section. The origin point was defined as the intersection of this linear regression with the x axis. Only measurements obtained before the point where the medulla began to exhibit keratinization were used for the linear regression.

A von Bertalanffy growth curve was fitted between the tubule wall width values and the distance to the plate base to estimate the origin point. The medulla keratinization period was calculated as the time required for the tubules to achieve 95% of their asymptotic width.

Results

At the most proximal position of the baleen plate, the histological sections showed that the cortex had already started to undergo keratinization, while the medulla was only composed of soft connective tissue (Fig 3a). In this region, the two components were separated by a third layer (Fig 3a; arrows) composed of two types of cells: flat keratinized cells near the cortex and round keratin-free cells near the medulla. Although the third layer formed a flat edge at its border with the cortex, at the border with the medulla, it formed evaginations that penetrated the medulla (Fig 3a; arrows). The three-layer structure occurred approximately along the first 7.3 ± 3 cm of the plate, which was well within the “gum” region. Along this segment, the cortex progressively increased in thickness linearly when advancing distally (Fig 4). When this segment ended, approximately 3-8 cm before the baleen emerged from the “gum”, the structure abruptly changed. The layer between the cortex and the medulla formed filaments that crossed the medulla, dividing it into small sections (Fig 3b). These sections eventually became the walls of the tubules in the mature medulla (Fig 3c). In addition, the growth rate of the cortex was abruptly reduced by approximately 3 cm, after which its width stabilized (Fig 4).

As the baleen plate grew, the tubule walls became thicker. Some concentric dark rings appeared around the lumen of the tubules (Fig 3d; arrows) which had been previously identified as calcium rings by Pfeiffer (1992). The enlargement and keratinization of the tubule walls extended for approximately 20.65 ± 7.04 cm (Table

1) and ended well after the baleen plate had emerged from the “gum”. Finally, during this stage, some pigment granules appeared in the medulla and became more frequent in the older parts of the plate (Fig 3d; arrows).

The “gum” was approximately 12 cm thick. Once the baleen plate emerged from it, the cortex started to become eroded (Fig 4). The connective tissue inside the tubules, which was always present under the “gum”, remained in the first emerged centimetres but eventually disappeared. However, its disappearance may have been enhanced by the sectioning process given that some left-over tissue is sometimes present at positions situated more distally (Fig 3e; arrows). This may indicate that the connective tissue is more loosely attached to the tubule walls in the more distal positions. In the fully formed tubules, the lumen appeared empty or filled with either a vacuole (or possibly cellular debris (Szewciw et al., 2010)) or keratin (Fig 3f; arrows).

The $\delta^{15}N$ values followed one sinusoid oscillation along the 20 cm of sampled baleen plate in both the cortex and the medulla (Fig 5). However, the amplitude of the variation of the $\delta^{15}N$ values was approximately 78 % higher in the cortex than in the medulla (Table 1). The cross-correlation of the two $\delta^{15}N$ values showed that the medulla values were 5 ± 1.6 cm lagged (equivalent to three months according to a growth rate of 20 $cm \cdot year^{-1}$) related to the corresponding values in the cortex (Table 1).

Discussion

The histological examination confirmed that the baleen plate was keratinized from the outside in (Pinto and Shadwick, 2013). It also showed that the cortex formed first and that its origin point was at the very base of the baleen plate. Once the baleen plate emerged from the “gum” the width of the cortex decreased, possibly due to erosion (Werth et al., 2016). While the synthesis of the cortex was linear and fast, the synthesis of the medulla was slow and the increase in tubule thickness fit a von Bertalanffy growth curve.

The present results are relevant to studies involving stable isotope analysis because the dissimilar processes of the formation of the cortex and the medulla are likely to result in different stable isotope values depending on which component of the baleen plate is subsampled. In other words, the shorter growth period of the cortex compared to that of the medulla reduces the period during which the cortex integrates stable isotopic information. This likely increases the resolution of the cortex time-series

record, which in turn increases the amplitude of the $\delta^{15}N$ oscillations. On the other hand, the long period required for the medulla integration would act as a moving average point, which would dampen the variability of the isotopic signal. In addition, the difference in location along the baleen plate of the origin point of the two components produces a lag, equivalent to a 3-month lag, between the $\delta^{15}N$ values of the medulla with respect to those of the cortex. We expected this lag to be the same as the distance existing between the respective origin points of each component, but we found in all cases that it was slightly shorter than that distance. The reason for this finding was unclear, but it may have been an artefact associated with the model fitted to calculate the growth period of the cortex. We assumed that the cortex grew following a linear model because the scant number of points that we had available showed this tendency. However, we suspect that, for a greater number of points/samples, a von Bertalanffy model would be more adequate and would likely place the origin point of the cortex closer to that of the medulla.

Although baleen plates have a clear curvature in their growth axis (Fig 2), the cuts performed with the circular saw were all straight cuts. This is likely to produce an error in the measurements that would become larger in the ventral samples, where the curvature becomes more pronounced (Fig 2). This error would cause a lower measured distance between the subsample and the base of the plate and would distort the histological examination since the sections would no longer be perfectly perpendicular to the growth axis. However, it should be noted that none of these errors would greatly impact our study because most of the measurements and the conclusions have been extracted from the synthesis zone of the plate, where the curvature is minimal.

These findings emphasize the need for standardization of the subsampling methods used in baleen plate stable isotope studies. Clearly, samples should be taken only from one layer, either the cortex or the medulla, and should never be collected as a combination of the two components. This is quite easy to achieve since the two histological components can be distinguished visually during the subsampling. After considering the two options, we recommend that the cortex should preferentially be analysed rather than the medulla for two reasons: a) it is close to the surface and is therefore easier to sample, and b) it integrates a shorter period, likely making its resolution in recording the stable isotope ratios higher. The increase in resolution not only provides a sharper picture of the migratory pattern, but also more accurate stable

isotope values, something which is especially important when estimating diet or feeding grounds based on the stable isotope ratios. For example, an error in 1 ‰ in the $\delta^{15}N$ values would mask any potential difference between segments of the baleen plate deposited for example in Greenland and NW Spain (McMahon et al., 2013). Additionally, we strongly recommend starting the subsampling as far in the dorsal direction as possible and including the zone located underneath the “gum” because this is where the most recent stable isotope values (i.e., the origin point) are located.

However, this method involves a caveat related to the erosion suffered by the cortex layer once it emerges from the “gum” (Werth et al., 2016). As the cortex erodes, deeper layers of the cortex become exposed to the surface, and at the very tip of the baleen plate, only the cortex layer closest to the medulla will remain. Since the cortex closest to the medulla is synthesised after the cortex closest to the surface, it is expected that there will be a small lag between the respective isotope ratio values. The overall effect of this caveat would be a slight expansion of all the stable isotope oscillations in the baleen plate, which may somewhat skew the measurements of the growth rate. It is not clear how this error may be distributed along the baleen since different parts of the baleen may suffer different amounts of erosion. It is suspected that the zones with high erosion rates may also exhibit greater expansion of stable isotope oscillation.

Although this study was based on the results from only two baleen plates from two different individuals, we believe that its results are representative of the species because the synthesis of a tissue is a highly conservative process and tends to follow the same pattern within species. On the same grounds, we believe that the process is not affected by the age, sex or any other biological trait of the individual. Also, given that the baleen plate is a fully keratinized tissue, and that keratin does not experience changes or decomposition if properly stored, we consider that the conclusions apply to specimens properly stored in museum collections, irrespectively of their age.

Furthermore, the fact that the overall structure of the baleen plate is similar in blue (Fudge et al., 2009; Van Utrecht, 1966), minke, humpback, sei (Szewciw et al., 2010) and fin whales (Pinto and Shadwick, 2013; Van Utrecht, 1966) supports the idea that the above findings and recommendations are also applicable to other balaenopterid species. However, before the present results are extended to other species, it is recommended that confirmation studies be conducted because some small differences in the structure of the plate, particularly in the pattern of calcification or in the

distribution of the tubules, are known to occur between species (Szewciw et al., 2010). Conversely, the plate of balaenids is much thicker and longer, and its pattern of formation may therefore not be directly comparable. Moreover, the above considerations may likely apply to other elements and molecules, such as heavy metals (Hobson et al., 2004) and hormones (Hunt et al., 2016), whose analyses can also be carried out in baleen plates. The only exception to this situation would be for elements that are progressively adsorbed into the plate from the surrounding seawater, as occurs for strontium (Vighi et al., 2019).

Acknowledgements

The baleen plates used in this study were provided by the Marine and Freshwater Research Institute of Iceland (MFRI). The authors are grateful to the staff of the MFRI who conducted the fieldwork and to Kristján Loftsson, who kindly provided facilities to conduct sampling at the Hvalur whaling station. The stable isotope analyses were conducted at the *Centres Científics i Tecnològics* (CCiT-UB) of the University of Barcelona. The authors would like to thank Mercè Durfort i Coll and Jordi Correas Romero for their support and expertise during the sampling and interpretation of the histological work. This project was supported by project CGL2015-70468-R (MINECO/FEDER, UE). DR conducted the experiments as part of his PhD work, which was funded by the Ministerio de Ciencia Innovación y Universidades of the Spanish Government.

Literature cited

Aguilar, A., Giménez, J., Gómez-Campos, E., Cardona, L., Borrell, A., 2014. $\delta^{15}N$ value does not reflect fasting in mysticetes. PLoS One 9, e92288. https://doi.org/10.1371/journal.pone.0092288

Ayliffe, L.K., Cerling, T.E., Robinson, T., West, A.G., Sponheimer, M., Passey, B.H., Hammer, J., Roeder, B., Dearing, M.D., Ehleringer, J.R., 2004. Turnover of carbon isotopes in tail hair and breath CO_2 of horses fed an isotopically varied diet. Oecologia 139, 11–22. https://doi.org/10.1007/s00442-003-1479-x

Bentaleb, I., Martin, C., Vrac, M., Mate, B., Mayzaud, P., Siret, D., De Stephanis, R., Guinet, C., 2011. Foraging ecology of Mediterranean fin whales in a changing environment elucidated by satellite tracking and baleen plate stable isotopes. Mar. Ecol. Prog. Ser. 438, 285–302. https://doi.org/10.3354/meps09269

Bond, A.L., Hobson, K.A., 2012. Reporting stable-isotope ratios in ecology:

372 recommended terminology, guidelines and best practices. Waterbirds 35, 324–
373 331. https://doi.org/10.1675/063.035.0213
374 Bond, A.L., Jardine, T.D., Hobson, K.A., 2016. Multi-tissue stable-isotope analyses
375 can identify dietary specialization. Methods Ecol. Evol. 7, 1428–1437.
376 https://doi.org/10.1111/2041-210X.12620
377 Bowen, G.J., Wassenaar, L.I., Hobson, K.A., 2005. Global application of stable
378 hydrogen and oxygen isotopes to wildlife forensics. Oecologia 143, 337–348.
379 https://doi.org/10.1007/s00442-004-1813-y
380 Busquets-Vass, G., Newsome, S.D., Calambokidis, J., Serra-Valente, G., Jacobsen,
381 J.K., Aguíñiga-García, S., Gendron, D., 2017. Estimating blue whale skin
382 isotopic incorporation rates and baleen growth rates: Implications for assessing
383 diet and movement patterns in mysticetes. PLoS One 12, 1–25.
384 https://doi.org/https://doi.org/10.1371/journal.pone.0177880
385 Clementz, M., Koch, P., 2001. Differentiating aquatic mammal habitat and foraging
386 ecology with stable isotopes in tooth enamel. Oecologia 129, 461–472.
387 https://doi.org/10.1007/s004420100745
388 DeHart, P.A.P., Picco, C.M., 2015. Stable oxygen and hydrogen isotope analyses of
389 bowhead whale baleen as biochemical recorders of migration and arctic
390 environmental change. Polar Sci. 9, 235–248.
391 https://doi.org/10.1016/j.polar.2015.03.002
392 Eisenmann, P., Fry, B., Holyoake, C., Coughran, D., Nicol, S., Bengtson Nash, S.,
393 2016. Isotopic evidence of a wide spectrum of feeding strategies in Southern
394 hemisphere humpback whale baleen records. PLoS One 11, 1–21.
395 https://doi.org/10.1371/journal.pone.0156698
396 Fry, B., Arnold, C., 1982. Rapid 13C / 12C turnover during growth of brown shrimp
397 (*Penaeus aztecus*). Oecologia 54, 200–204. https://doi.org/10.1007/BF00378393
398 Fudge, D.S., Szewciw, L.J., Schwalb, A.N., 2009. Morphology and development of
399 blue whale baleen: An annotated translation of Tycho Tullberg's classic 1883
400 paper. Aquat. Mamm. 35, 226–252. https://doi.org/10.1578/AM.35.2.2009.226
401 García-Vernet, R., Sant, P., Vikingsson, G.A., Borrell, A., Aguilar, A., 2018. Are
402 stable isotope ratios and oscillations consistent in all baleen plates along the
403 filtering apparatus? Validation of an increasingly used methodology. Rapid
404 Commun. Mass Spectrom. 32, 1257–1262. https://doi.org/10.1002/rcm.8169
405 Giménez, J., Gómez-Campos, E., Borrell, A., Cardona, L., Aguilar, A., 2013. Isotopic

406 evidence of limited exchange between Mediterranean and eastern North Atlantic
407 fin whales. Rapid Commun. Mass Spectrom. 27, 1801–1806.
408 https://doi.org/10.1002/rcm.6633
409 Hobson, K.A., 1999. Tracing origins and migration of wildlife using stable isotopes: A
410 review. Oecologia 120, 314–326. https://doi.org/10.1007/s004420050865
411 Hobson, K.A., Riget, F.F., Outridge, P.M., Dietz, R., Born, E., 2004. Baleen as a
412 biomonitor of mercury content and dietary history of North Atlantic Minke Whales
413 (*Balaenoptera acutorostrata*): Combining elemental and stable isotope
414 approaches. Sci. Total Environ. 331, 69–82.
415 https://doi.org/10.1016/j.scitotenv.2004.03.024
416 Hobson, K.A., Schell, D.M., 1998. Stable carbon and nitrogen isotope patterns in
417 baleen from eastern Arctic bowhead whales (*Balaena mysticetus*). Can. J. Fish.
418 Aquat. Sci. 55, 2601–2607. https://doi.org/10.1139/cjfas-55-12-2601
419 Hunt, K.E., Lysiak, N.S., Moore, M.J., Rolland, R.M., 2016. Longitudinal
420 progesterone profiles in baleen from female North Atlantic right whales
421 (*Eubalaena glacialis*) match known calving history. Conserv. Physiol. 4, 1–9.
422 https://doi.org/10.1093/conphys/cow014
423 Matthews, C.J.D., Ferguson, S.H., 2015. Seasonal foraging behaviour of eastern
424 Canada-West Greenland bowhead whales: An assessment of isotopic cycles
425 along baleen. Mar. Ecol. Prog. Ser. 522, 269–286.
426 https://doi.org/10.3354/meps11145
427 McMahon, K.W., Hamady, L.L., Thorrold, S.R., 2013. A review of ecogeochemistry
428 approaches to estimating movements of marine animals. Limnol. Oceanogr. 58,
429 697–714.
430 Mitani, Y., Bando, T., Takai, N., Sakamoto, W., 2006. Patterns of stable carbon and
431 nitrogen isotopes in the baleen of common minke whale *Balaenoptera*
432 *acutorostrata* from the western North Pacific. Fish. Sci. 72, 69–76.
433 https://doi.org/10.1111/j.1444-2906.2006.01118.x
434 Peterson, B.J., Fry, B., 1987. Stable isotopes in ecosystem studies. Annu. Rev. Ecol.
435 Syst. 18, 293–320.
436 https://doi.org/https://doi.org/10.1146/annurev.es.18.110187.001453
437 Pfeiffer, C.J., 1992. Cellular structure of terminal baleen in various mysticete species.
438 Aquat. Mamm. 18, 67–73.
439 Pinto, S.J.D., Shadwick, R.E., 2013. Material and structural properties of fin whale

(*Balaenoptera physalus*) zwischensubstanz. J. Morphol. 274, 947–955. https://doi.org/10.1002/jmor.20154

R Core Team, 2016. R: A language and environment for statistical computing. R Foundation for Statistical Computing, Vienna, Austria. URL https://www.R-project.org/.

Rice, D.W., 2002. Baleen, in: Perrin, W.F., Würsig, B., Thewissen, J.G.M. (Eds.), Encyclopedia of Marine Mammals. Elsevier-Academic Press., Amsterdam (Netherland), pp. 61–62.

Rita, D., Drago, M., Galimberti, F., Cardona, L., 2017. Temporal consistency of individual trophic specialization in southern elephant seals Mirounga leonina. Mar. Ecol. Prog. Ser. 585, 229–242. https://doi.org/https://doi.org/10.3354/meps12411

Rubenstein, D.R., Hobson, K.A., 2004. From birds to butterflies: Animal movement patterns and stable isotopes. Trends Ecol. Evol. 19, 256–263. https://doi.org/10.1016/j.tree.2004.03.017

Ryan, C., McHugh, B., Trueman, C.N., Sabin, R., Deaville, R., Harrod, C., Berrow, S.D., O'Connor, I., 2013. Stable isotope analysis of baleen reveals resource partitioning among sympatric rorquals and population structure in fin whales. Mar. Ecol. Prog. Ser. 479, 251–261. https://doi.org/10.3354/meps10231

Skrzypek, G., 2013. Normalization procedures and reference material selection in stable HCNOS isotope analyses: An overview. Anal. Bioanal. Chem. 405, 2815–2823. https://doi.org/10.1007/s00216-012-6517-2

Szewciw, L.J., de Kerckhove, D.G., Grime, G.W., Fudge, D.S., 2010. Calcification provides mechanical reinforcement to whale baleen alpha-keratin. Proc. R. Soc. Ser. B, Biol. Sci. 277, 2597–2605. https://doi.org/10.1098/rspb.2010.0399

Van Utrecht, W.L., 1966. On the growth of the baleen plate of the fin whale and the blue whale. Bijdr. tot Dierkd. 35, 3–38.

Vighi, M., Borrell, A., Víkingsson, G., Gunnlaugsson, T., Aguilar, A., 2019. Strontium in fin whale baleen: A potential tracer of mysticete movements across the oceans? Sci. Total Environ. 650, 1224–1230. https://doi.org/10.1016/j.scitotenv.2018.09.103

Werth, A.J., Straley, J.M., Shadwick, R.E., 2016. Baleen wear reveals intraoral water flow patterns of mysticete filter feeding. J. Morphol. 277, 453–471. https://doi.org/10.1002/jmor.20510

474 Young, S., Deméré, T.A., Ekdale, E.G., Berta, A., Zellmer, N., 2015. Morphometrics
475 and structure of complete baleen racks in gray whales (*Eschrichtius robustus*)
476 from the eastern North Pacific Ocean. Anat. Rec. 298, 703–719.
477 https://doi.org/10.1002/ar.23108

478

Tables

		$\delta^{15}N$ value amplitude (‰)		$\delta^{15}N$ value lag (cm)	Growth period (cm)	
Whale	Section	Cortex	Medulla	Cortex-medulla	Cortex	Medulla
81	Labial	3.15	1.31	5	6.1	25.5
81	Lingual	2.68	1.87	3	3.7	11.1
97	Labial	2.13	1.02	7	10.4	26.4
97	Lingual	1.75	1.46	5	9.2	19.6
Mean		2.43 ± 0.61	1.42 ± 0.35	5 ± 1.6	7.4 ± 3.0	20.7 ± 7.0

Table 1. Summary of the results for stable isotope ratios and histological measurements from the four baleen plates strips analysed.

Figures

All figures may appear as black/white in the printed version and in color in the online version.

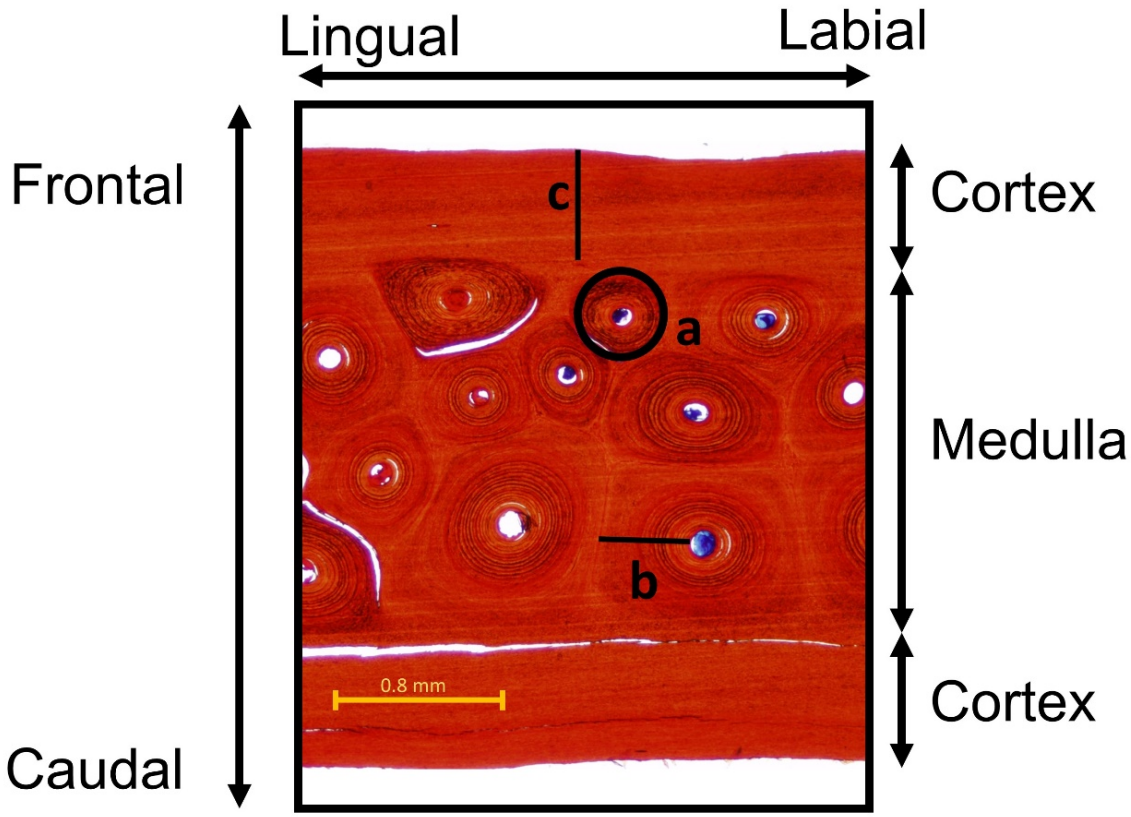

Fig. 1 Histological section of a fin whale baleen plate cut perpendicular to the growth axis of the plate (see orientation in Fig. 2). The image shows the three layers that constitute the plate: the two cortex layers and the medulla layer. The medulla layer is composed of horny tubules (a) that run parallel to the growth axis. The image also shows the two measurements used in this study: the width of the tubule wall (b) and the width of the cortex (c). A colour version of this figure can be found in the online version.

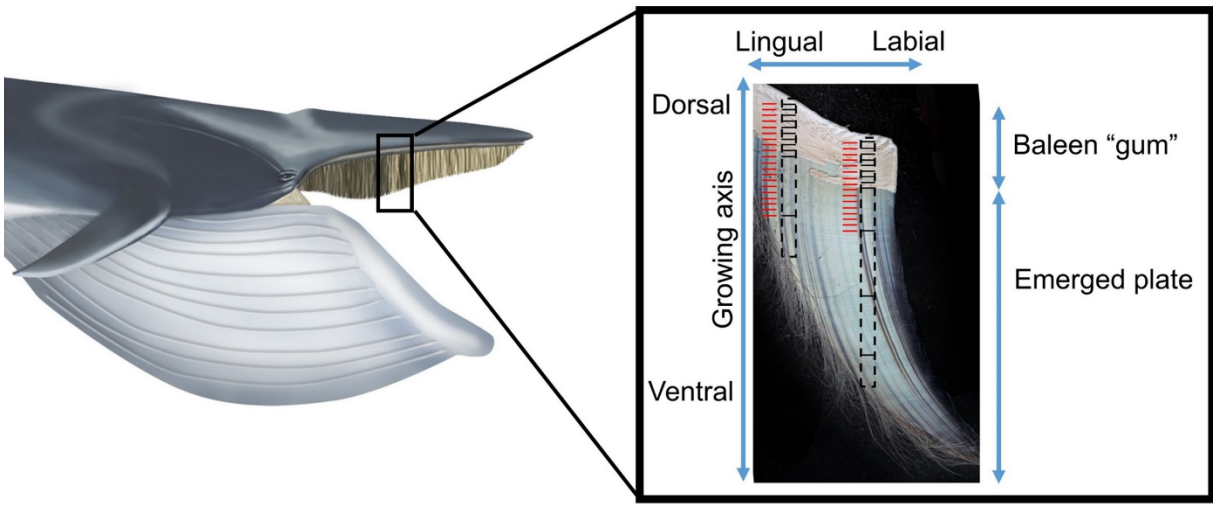

Fig. 2 Position of the baleen plates in vivo (left) and sampling scheme of the baleen plate (right). The white area in the dorsal zone of the plate is the baleen plate “gum” or zwischensubstanz. The dashed rectangles represent the 1 cm strips cut with the circular saw (not to scale). The red lines represent the stable isotope sampling points, and the black lines show the orientation of the samples used to obtain the histological sections. A colour version of this figure can be found in the online version.

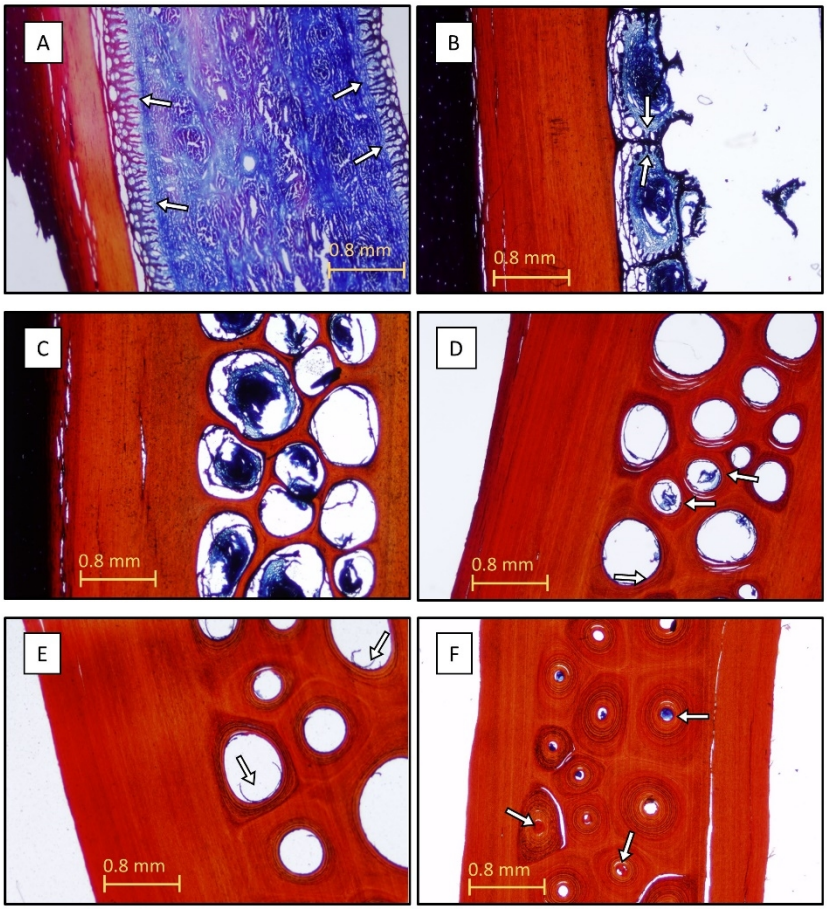

Fig. 3 Selection of photomicrographs of a baleen plate at different development stages. A shows the three-layer structure of the incipient plate: soft connective medulla (light blue), tissue between the cortex and the medulla (arrows) and cortex (orange); it also shows the "gum" (deep blue). B shows the segmented connective medulla with the evaginations facing the inside of the segments (arrows). C shows an incipient tubule with keratinized walls and a mature cortex. D shows the calcium rings and pigmentation granules around the tubules (arrows). E shows the cellular debris (arrows) inside the tubule lumen after the baleen plate has emerged from the "gum". F shows the cellular debris (arrows) inside the tubule lumen in the mature baleen plate. A colour version of this figure can be found in the online version.

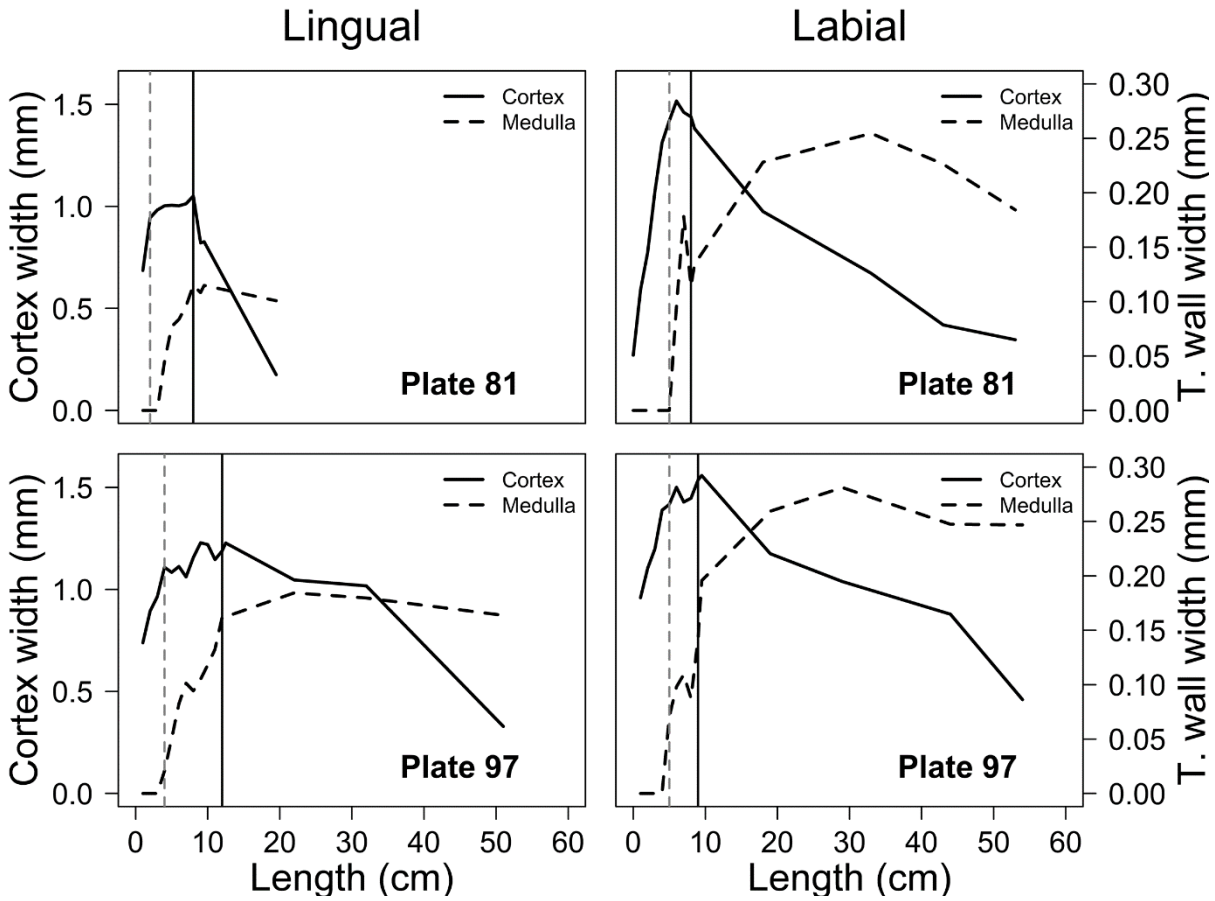

Fig. 4 Cortex and tubule wall width along the four baleen plate strips examined. The strips were extracted from the lingual (left) and labial (right) sides of the plates collected from whale #81 (top) and whale #97 (bottom). The dashed grey vertical line indicates the position at which the medulla starts to form. The continuous black vertical line indicates the position at which the plate emerges from the “gum”. Length was measured from the dorsal-most part of the plate (i.e., the point closest to the bone).

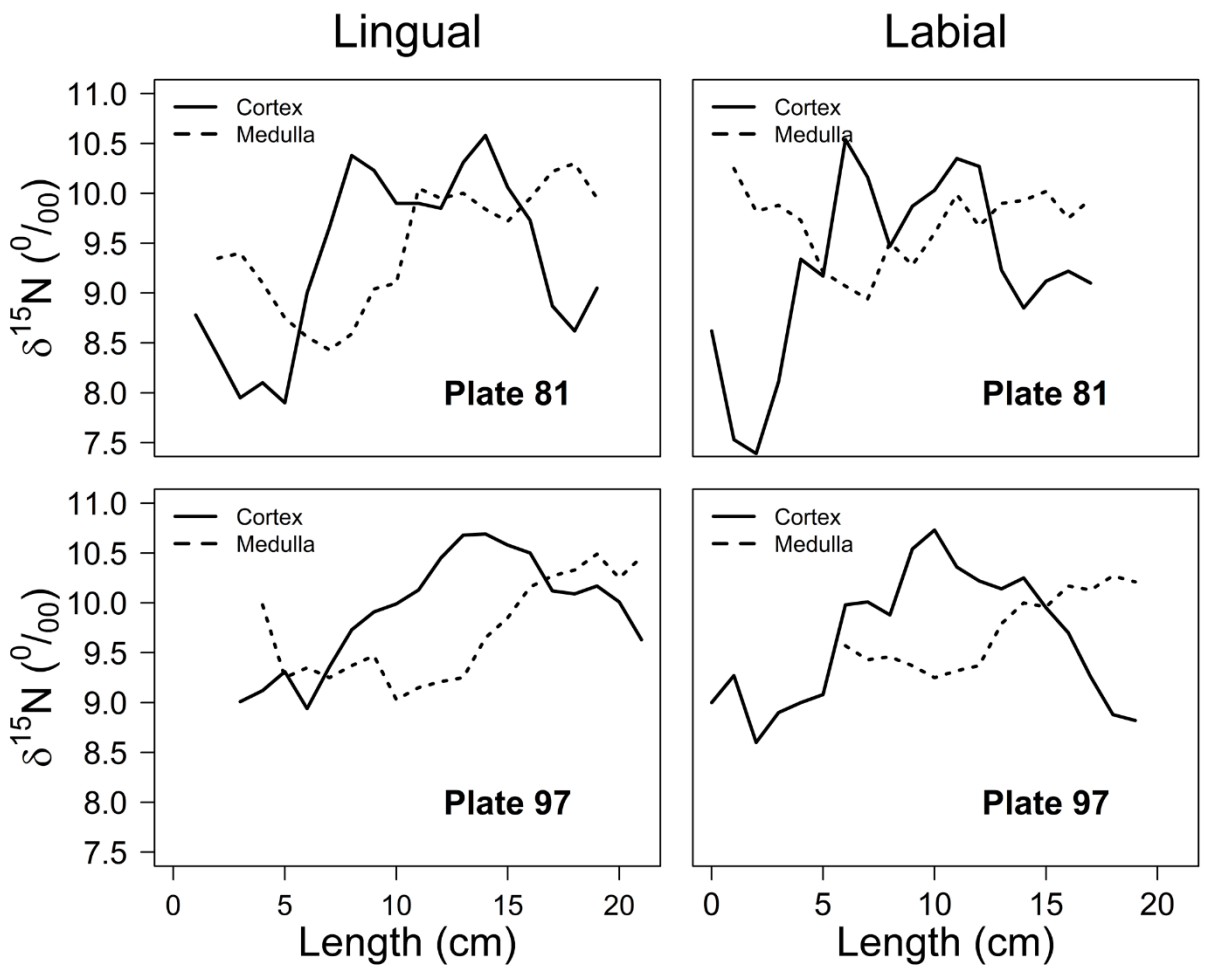

Fig. 5 Variation in the $\delta^{15}N$ values of the cortex and medulla along the four strips of baleen plates analysed. These strips correspond to the lingual (left) and labial (right) sides of plates from whales #81 (top) and #97 (bottom). Length was measured from the dorsal-most part of the plate (i.e., the point closest to the bone).

SD1. Detailed results of the cortex and medulla measurements. A minimum of 7 measurements were conducted for each sample and 20 measurements were conducted when possible.

Plate	Section	Distance from base (cm)	Cortex (mm)	Cortex SD	Lumen diameter (mm)	Lumen SD	Tubule wall diameter (mm)	Tubule wall SD
81	Lingual	1	0.686	0.153	0.000		0.000	
81	Lingual	2	0.944	0.041	0.000		0.000	
81	Lingual	3	0.983	0.032	0.000		0.000	
81	Lingual	4	1.003	0.054	0.220	0.033	0.310	0.056
81	Lingual	5	1.006	0.053	0.221	0.045	0.375	0.071
81	Lingual	6	1.003	0.042	0.170	0.035	0.338	0.062
81	Lingual	7	1.013	0.062	0.137	0.028	0.328	0.062
81	Lingual	8	1.051	0.110	0.120	0.026	0.350	0.058
81	Lingual	9	0.821	0.084	0.109	0.029	0.326	0.042
81	Lingual	9.5	0.827	0.150	0.107	0.023	0.337	0.071
81	Lingual	19.5	0.175	0.054	0.073	0.008	0.275	0.058
81	Labial	0	0.271	0.018	0.000		0.000	
81	Labial	1	0.590	0.032	0.000		0.000	
81	Labial	2	0.775	0.031	0.000		0.000	
81	Labial	3	1.074	0.038	0.000		0.000	
81	Labial	4	1.313	0.046	0.000		0.000	
81	Labial	5	1.420	0.043	0.000		0.000	
81	Labial	6	1.516	0.055	0.600	0.108	0.793	0.233
81	Labial	7	1.461	0.033	0.446	0.114	0.803	0.298
81	Labial	8	1.439	0.045	0.545	0.164	0.773	0.219
81	Labial	8.5	1.381	0.059	0.479	0.117	0.748	0.185
81	Labial	18	0.346	0.054	0.099	0.022	0.468	0.120
81	Labial	33	0.975	0.047	0.148	0.036	0.604	0.093
81	Labial	43	0.673	0.059	0.102	0.018	0.611	0.154
81	Labial	53	0.419	0.096	0.111	0.016	0.564	0.141
97	Lingual	1	0.739	0.095	0.000		0.000	
97	Lingual	2	0.894	0.100	0.000		0.000	
97	Lingual	3	0.964	0.087	0.342	0.080	0.000	
97	Lingual	4	1.109	0.046	0.357	0.075	0.399	0.081
97	Lingual	5	1.084	0.042	0.328	0.066	0.429	0.118
97	Lingual	6	1.113	0.058	0.301	0.091	0.466	0.117
97	Lingual	7	1.061	0.068	0.236	0.061	0.439	0.151
97	Lingual	8	1.156	0.047	0.246	0.065	0.435	0.088
97	Lingual	9	1.229	0.043	0.225	0.059	0.435	0.102
97	Lingual	10	1.220	0.061	0.210	0.055	0.447	0.124
97	Lingual	11	1.146	0.054	0.198	0.032	0.463	0.068
97	Lingual	12	1.189	0.055	0.176	0.046	0.500	0.087
97	Lingual	12.5	1.228	0.064	0.156	0.037	0.481	0.100
97	Lingual	22	1.046	0.050	0.118	0.049	0.486	0.090
97	Lingual	32	1.018	0.090	0.106	0.018	0.465	0.084
97	Lingual	51	0.329	0.140	0.088	0.022	0.415	0.070

97	Labial	1	0.959	0.029	0.000		0.000	
97	Labial	2	1.104	0.105	0.000		0.000	
97	Labial	3	1.199	0.086	0.000		0.000	
97	Labial	4	1.389	0.047	0.000		0.000	
97	Labial	5	1.418	0.052	0.569	0.199	0.710	0.211
97	Labial	6	1.501	0.072	0.564	0.082	0.760	0.090
97	Labial	7	1.429	0.069	0.465	0.102	0.684	0.154
97	Labial	8	1.447	0.063	0.391	0.115	0.566	0.122
97	Labial	9	1.538	0.057	0.424	0.108	0.710	0.149
97	Labial	9.5	1.559	0.049	0.343	0.091	0.734	0.178
97	Labial	19	1.175	0.094	0.144	0.037	0.663	0.188
97	Labial	29	1.039	0.058	0.116	0.017	0.679	0.143
97	Labial	44	0.879	0.077	0.109	0.033	0.604	0.104
97	Labial	54	0.460	0.089	0.105	0.019	0.599	0.114

SD2 Table. Raw data of the $\delta^{15}N$ and $\delta^{13}C$ of the cortex and medulla samples analysed.

Plate	Section	Distance from base (cm)	Cortex $\delta^{15}N$	Cortex $\delta^{13}C$	Medulla $\delta^{15}N$	Medulla $\delta^{13}C$
81	Lingual	1	8,78	-19,85		
81	Lingual	2	8,37	-20,10	9,35	-19,81
81	Lingual	3	7,95	-21,08	9,40	-19,92
81	Lingual	4	8,10	-20,43	9,10	-20,33
81	Lingual	5	7,90	-20,48	8,75	-20,14
81	Lingual	6	9,00	-19,64	8,56	-20,33
81	Lingual	7	9,66	-19,08	8,43	-20,54
81	Lingual	8	10,38	-18,81	8,59	-20,28
81	Lingual	9	10,23	-18,85	9,04	-19,64
81	Lingual	10	9,42	-18,78	9,10	-19,36
81	Lingual	11	9,93	-18,58	10,05	-18,98
81	Lingual	12	9,89	-18,30	9,95	-19,03
81	Lingual	13	10,31	-18,97	10,00	-18,72
81	Lingual	14	10,58	-18,69	9,84	-18,83
81	Lingual	15	10,06	-19,17	9,72	-18,65
81	Lingual	16	9,73	-18,41	9,95	-18,59
81	Lingual	17	8,87	-18,88	10,22	-18,62
81	Lingual	18	8,62	-19,18	10,30	-18,46
81	Lingual	19	9,05	-19,87	9,95	-18,29
81	Labial	0	8,62	-20,62		
81	Labial	1	7,53	-21,48	10,25	-18,85
81	Labial	2	7,39	-21,72	9,82	-19,46
81	Labial	3	8,11	-20,31	9,88	-19,58
81	Labial	4	9,34	-19,49	9,73	-19,76

81	Labial	5	9,17	-19,85	9,21	-20,33
81	Labial	6	10,54	-19,48	9,07	-20,34
81	Labial	7	10,16	-19,29	8,94	-20,18
81	Labial	8	9,47	-19,24	9,51	-19,60
81	Labial	9	9,87	-19,11	9,28	-19,55
81	Labial	10	10,03	-19,51	9,60	-19,54
81	Labial	11	10,35	-19,47	9,99	-19,14
81	Labial	12	10,27	-19,10	9,67	-19,08
81	Labial	13	9,23	-19,00	9,90	-19,07
81	Labial	14	8,85	-19,16	9,93	-19,01
81	Labial	15	9,12	-20,01	10,02	-18,97
81	Labial	16	9,22	-20,86	9,75	-19,11
81	Labial	17	9,10	-20,81	9,94	-19,07
97	Lingual	3	9,01	-18,84		
97	Lingual	4	9,12	-18,94	9,98	-19,50
97	Lingual	5	9,31	-18,59	9,25	-18,73
97	Lingual	6	8,94	-19,15	9,35	-18,22
97	Lingual	7	9,36	-19,41	9,25	-18,46
97	Lingual	8	9,73	-19,19	9,37	-18,66
97	Lingual	9	9,91	-19,20	9,47	-18,47
97	Lingual	10	9,99	-19,03	9,03	-18,51
97	Lingual	11	10,13	-18,89	9,15	-18,73
97	Lingual	12	10,45	-18,89	9,21	-18,63
97	Lingual	13	10,68	-18,77	9,25	-18,53
97	Lingual	14	10,69	-18,88	9,65	-18,62
97	Lingual	15	10,58	-18,81	9,85	-18,55
97	Lingual	16	10,50	-18,76	10,16	-18,46
97	Lingual	17	10,12	-18,70	10,27	-18,19
97	Lingual	18	10,09	-18,47	10,33	-18,25
97	Lingual	19	10,17	-18,37	10,49	-18,21
97	Lingual	20	10,01	-18,27	10,25	-18,23
97	Lingual	21	9,63	-18,35	10,46	-18,01
97	Labial	0	9,00	-18,74		
97	Labial	1	9,27	-19,15		
97	Labial	2	8,63	-18,99		
97	Labial	3	8,87	-19,02		
97	Labial	4	8,97	-19,11		
97	Labial	5	9,08	-19,16		
97	Labial	6	9,98	-19,06	9,57	-18,66
97	Labial	7	10,01	-18,98	9,43	-18,27
97	Labial	8	9,88	-18,88	9,46	-18,47
97	Labial	9	10,54	-18,65	9,37	-18,65
97	Labial	10	10,73	-18,68	9,25	-18,70
97	Labial	11	10,36	-18,61	9,32	-18,78
97	Labial	12	10,22	-18,65	9,42	-18,58
97	Labial	13	10,14	-18,47	9,89	-18,59

97	Labial	14	10,25	-18,45	10,00	-18,54
97	Labial	15	9,95	-18,25	9,96	-18,58
97	Labial	16	9,70	-18,26	10,17	-18,41
97	Labial	17	9,26	-18,59	10,13	-18,37
97	Labial	18	8,88	-18,92	10,27	-18,31
97	Labial	19	8,82	-18,85	10,21	-18,23